ACS OMEGA

http://pubs.acs.org/journal/acsodf

Article

Green Orange Peel-Mediated Bioinspired Synthesis of Nanoselenium and Its Antibacterial Activity against Methicillin-Resistant *Staphylococcus aureus*

Trung Dang-Bao, Thanh Gia-Thien Ho, Ba Long Do, Nguyen Phung Anh, Thi Diem Trinh Phan, Thi Bao Yen Tran, Nhat Linh Duong, Phan Hong Phuong,* and Tri Nguyen*

Cite This: *ACS Omega* 2022, 7, 36037−36046

Read Online

ACCESS | Metrics & More | Article Recommendations

ABSTRACT: In this study, green orange peel (GOP) was feasibly evidenced in preparing selenium nanoparticles (SeNPs). Acting as reducing agents, polyphenolic compounds were extracted from GOP at the optimal extraction conditions (at 70 °C for 1.5 h, mass ratio of dried orange peel/distilled water of 5/100). The formation of SeNPs was observed at the wavelength range of 250−300 nm by ultraviolet−visible spectroscopy (UV−vis), and their highest yield could be reached at the following conditions: volume ratio of extract/selenious acid solution (V_{Ext}/V_{Se}) of 40/10, synthesis duration of 4 h, selenious acid concentration (C_{Se}) of 80 mM, and reaction temperature of 120 °C. The highly crystalline structure of SeNPs in the hexagonal phase was characterized by powder X-ray diffraction (XRD) with a lattice parameter of 4.3 Å; meanwhile, their spheres with an average crystal size of 18.3 nm were estimated by high-resolution transmission electron microscope (HR-TEM). The rationale of bioreducing agents extracted from green orange peel for the formation of SeNPs was also recognized by Fourier-transform infrared spectroscopy (FT-IR). The antibacterial investigation of the SeNP sample was assessed against antibiotic-resistant bacteria, typically methicillin-resistant *Staphylococcus aureus* (MRSA), by executing the zone of inhibition and the minimum inhibitory concentration (MIC) tests. The SeNP sample demonstrated excellent antibacterial activity with an average diameter of inhibition zones of 20.0 ± 0.7 mm and an MIC of 4.94 μg/L. A comparison of the physicochemical properties of SeNPs synthesized from GOP extract by the hydrothermal method with SeNP products from other green reducing agents and other methods as well as its antibacterial activity compared with other nanoparticles and some antibiotics was conducted to highlight the superiority of GOP-mediated green-synthesized SeNPs.

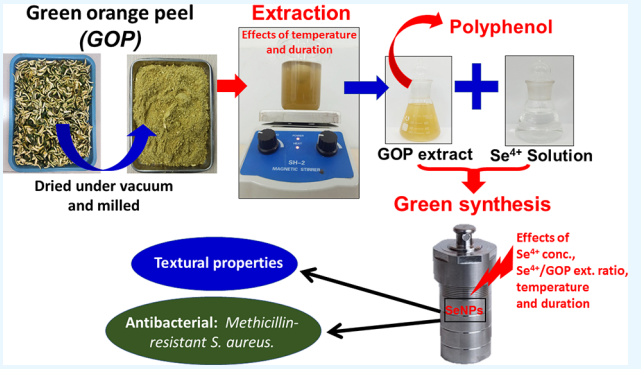

INTRODUCTION

Selenium is a practically useful element in the medical, antibacterial, antifungal, electronic, ceramic, metallurgical, and glass industries due to its unique chemical and physical properties.[1−3] Compared with traditional selenium compounds, nanoselenium has more unique properties, higher activity, and lower toxicity.[4] Especially, selenium nanoparticles (SeNPs) are investigated as new antibacterial agents since they are comparable in efficacy and even more powerful compared with conventional antibiotics.[5,6] Besides, much fewer new antibiotics have been introduced by the pharmaceutical industry, and none of them have enhanced activity against multiresistant bacteria. Methicillin-resistant *Staphylococcus aureus* (MRSA) is an antibiotic-resistant kind of *Staphylococcus aureus* that is typically resistant to beta-lactam antibiotics such as cephalosporin and penicillin (oxacillin and methicillin).[7] Various antibiotics, such as co-trimoxazole, fusidic acid, clindamycin, and mupirocin, are also utilized as a second-line option in treating MRSA.[8] But, these antibiotics can only be prescribed when there is no other alternative available because of the resistance risk. Alternative treatments against MRSA without the use of different antibiotic classes are extremely required. So, SeNPs are considered an effective solution for inhibiting drug-resistant bacteria. Therefore, the synthetic strategies and biological effects of SeNPs have been constantly explored for antibacterial purposes.

In general, the SeNP preparation focuses on the physical method, chemical reduction, and biosynthesis.[9,10] In the

Received: August 25, 2022
Accepted: September 21, 2022
Published: September 30, 2022

physical method, mechanical measures are usually related to extrusion, friction, ultrasound, impact, shear on solid raw materials, or sublimation condensation is assumed to change the intermolecular force of selenium to obtain SeNPs. In spite of the fast and straightforward approach, it has strict requirements for equipment conditions, the obtained SeNPs are of low purity, and their crystalline particle sizes are poorly controlled. In the chemical reduction, external reducing agents were added to the selenious acid solutions or sodium selenite to deliver SeNPs, such as ferrous iron,[11] hydroquinone,[12] sodium thiosulfate,[13] hydrazine,[14] silk fibroin,[15] ascorbic acid,[16] glucose,[17] and polysaccharides.[18] Nevertheless, this method requires harsh conditions and multiple steps involved in the preparation. Besides, the reducing agent, stabilizer, and template agent used in the synthesis are frequently harmful, as well as the secondary pollutants generated from chemical reactions.[19]

In recent years, eco-friendly and nontoxic approaches have been studied for SeNP biosynthesis using various microorganisms such as yeast, bacteria, and fungi[20−22] as well as plant extracts as reducing agents.[1,23,24] The size, morphology, and properties of SeNPs can be controlled by the incubation reaction duration, temperature, metallic ion concentration, initial pH solution, and the type of used microorganism. Practically, SeNP biosynthesis was performed on different bacteria such as *Lactobacillus acidophilus*,[25] *Bacillus subtilis*,[26] and probiotic lactic acid bacteria.[27] Besides, plant extracts derived from leaves, roots, fruits, and peels containing polyphenols, flavonoids, ascorbic acid, citric acids, carotenoids, etc., were also utilized as natural reducing and stabilizing agents for SeNP biosynthesis,[1,23,24,28] such as broccoli,[29] fenugreek extract,[30] parsley leaf,[31] dried *Vitis vinifera*,[32] *Terminalia arjuna* leaves,[33] *Clausena dentata*,[34] lemon juice,[4] and *Aloe vera* leaf.[35]

Green orange is one of the world's largest fruit crops, with a global production of millions of tons.[36] A large portion of this production is used to extract citrus juice, which leads to vast amounts of residues, including peel and segment membranes. Peels represent between 40 and 50% of the total weight of the fruits and remain as the primary byproduct. This byproduct is rich in polyphenolics, bioflavonoids, proteins, etc., that have been evidenced as reducing and stabilizing agents for nanomaterial synthesis.[19,37] In particular, polyphenolic compounds have been paid more and more attention due to their important biological activities, such as antibacterial, antioxidant, and anti-inflammatory activities.[38] Therefore, it is necessary to optimize the extraction conditions, obtaining the highest polyphenol content in the green orange peel (GOP) to enhance the efficiency of the SeNP biosynthesis, which has been less explored.

In this study, SeNPs were synthesized by reducing the Se^{4+} ion from a selenious acid solution using GOP extract as a reducing agent. The effect of conditions of GOP extraction, including duration and temperature, on the obtained polyphenol concentration was investigated. The operation parameters on the SeNP formation and its antibacterial activity against MRSA were also evaluated.

EXPERIMENTAL SECTION

Synthesis of Selenium Nanoparticles. After washing and shredding, GOP was dried to a constant weight at a temperature of 60 °C for 12 h. Then, 50 g of dried GOP was blended with 1 L of distilled water and heated to different temperature levels (60−80 °C) for various durations (1−3 h) under stirring. Finally, the orange peel extract was filtered and kept at 4 °C for further experiments. Selenious acid (H_2SeO_3, >99.9%), gallic acid ($C_6H_2(OH)_3COOH$, >97.5%), and the Folin−Ciocalteu phenol reagent were purchased from Merck.

The polyphenol concentration in the GOP extract was determined by the colorimetric method using the Folin−Ciocalteu reagent with gallic acid selected as the calibration standard.[39] The presence of polyphenol in the solution was determined by a UV−vis spectrophotometer (UV-1800, Shimadzu) at a wavelength of 760 nm.

To synthesize SeNPs, V_{Ext} (mL) of the GOP extract was mixed with V_{Se} (mL) of H_2SeO_3 solution with C_{Se} (mM) under stirring at 300 rpm for 30 min at room temperature to deliver a homogeneous solution. After stirring, the solution was transferred to a Teflon autoclave for hydrothermal treatment at T °C for t h. Effects of the volume ratio of extract/selenious acid solution (V_{Ext}/V_{Se}), the selenious acid concentration (C_{Se}), the duration time (t), and the synthesis temperature (T) on the formation of SeNPs were investigated to determine the best conditions.

Characterization of Selenium Nanoparticles. A UV−vis spectrometer (UV-1800, Shimadzu) was used to observe SeNP formation at 200−800 nm. The samples were diluted five times before being analyzed. The crystalline structure of the SeNP powder was determined by XRD analysis using a Bruker D2 Phaser powder diffractometer with Cu Kα radiation of 1.5406 nm wavelength at 40 kV and 30 mA in the range of 2θ angles 10−80° and a step size of 0.02°/s. The functional groups in the GOP extract on SeNPs were explored by FT-IR spectroscopy using an active Tensor 27-Bruker spectrometer with a scanning angle from 400 to 4000 cm^{-1}. The morphology and nanosize of SeNP samples were estimated by HR-TEM analysis on a JEOL JEM2100 instrument. The element analysis of SeNP samples was performed by energy-dispersive X-ray (EDX) spectroscopy on a Horiba-7593 instrument.

Antibacterial Activity. The agar disk diffusion method was employed to determine a zone of inhibition against MRSA. The agar medium after autoclaving and drying was inoculated with liquid overnight MRSA culture to a cell density of 5×10^5 CFU/mL. Once the agar was solidified, the wells were punched in the agar and filled with 10 μL of the SeNP solution. The plates then were photographed, and the inhibition zone diameter was measured after incubation for 24 h at 37 °C. All the investigations were run in triplicate, and the average result was taken.

The MIC value of the SeNP samples against MRSA was determined using the dilution method. To evaluate the MIC, various concentrations ($N/2$, $N/4$, $N/8$, $N/16$, $N/32$, $N/64$, $N/128$, $N/256$, $N/512$, $N/1024$, and $N/2048$, with N being the initial concentration, N = 1.263 g/L) of the SeNP solution were tested against MRSA. Then, 10 μL of MRSA was added to different plates containing different concentrations of the SeNP solutions mentioned above, and the plates were incubated at 37 °C for 24 h. The lowest concentration inhibiting visual growth of MRSA, indicated by increased turbidity, is considered the MIC value.

RESULTS AND DISCUSSION

The Suitable Extraction of Green Orange Peel. The effects of temperature and duration on the polyphenol yield were examined, showing the highest polyphenol yield of 13.5 ±

https://doi.org/10.1021/acsomega.2c05469
ACS Omega 2022, 7, 36037−36046

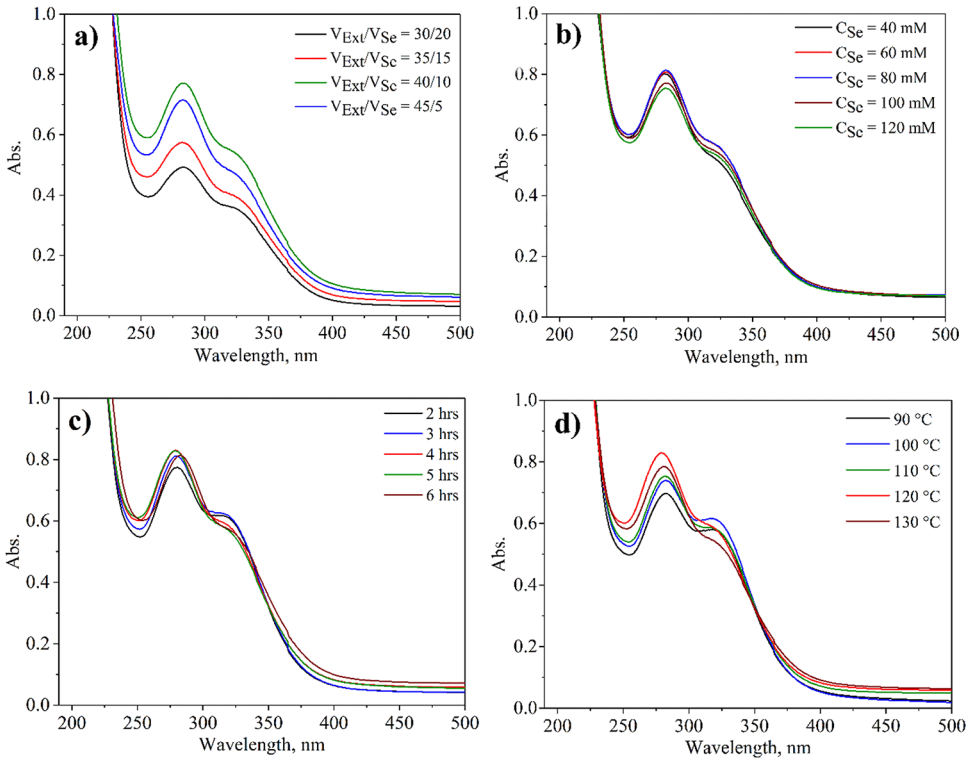

Figure 1. UV−vis spectra of SeNP solutions synthesized under various conditions: (a) effect of V_{Ext}/V_{Se} volume ratio; (b) effect of H_2SeO_3 concentration; (c) effect of temperature; and (d) effect of synthesis duration.

0.2 mg/g extracted at 70 °C for 1.5 h using the mass ratio of dried orange peel/distilled water of 5/100. At lower temperatures and shorter times, polyphenolic compounds were not absolutely extracted.[40,41] Theoretically, plant tissues are softened, and weak interactions affect cell membranes under high temperatures; thus, polyphenol compounds can be easily extracted into water.[42] However, if the process takes place at high temperatures for too long, these compounds are susceptible to chemical changes due to their unstable nature,[43,44] leading to decreasing process efficiency. Therefore, the extraction conditions to obtain polyphenols were determined as 70 °C for 1.5 h.

The Green Synthesis of Selenium Nanoparticles. The influence of the operation parameters on the SeNP synthesis yield was investigated by UV−vis spectral analysis (Figure 1), showing the SeNP formation observed in the wavelength range of 250−300 nm. When the V_{Ext}/V_{Se} ratio increased from 30/20 to 35/15 and 40/10, the yield of SeNP formation increased; however, the absorbance of SeNPs decreased when this ratio increased up to 45/5 (Figure 1a). As analyzed above, polyphenols contained in the green orange peel extract played an important role in reducing Se^{4+} toward Se^0. Therefore, an increase of the extract fraction in agreement with an increase of polyphenols facilitated the reduction of metal ions, achieving a higher efficiency of SeNP formation. However, when this ratio increased to a certain level (45/5), the selenium concentration in the survey sample dropped, resulting in a decrease in the SeNP formation efficiency. Therefore, the V_{Ext}/V_{Se} ratio was chosen to be 40/10 for the subsequent investigations.

When the initial Se^{4+} concentration (C_{Se}) increased from 40 to 80 mM, the SeNP formation efficiency increased. At higher concentrations (100 and 120 mM), the intensity of SeNP plasmon sharply decreased (Figure 1b). At low concentrations, metal nanoparticles appeared with very low intensity; when increasing Se^{4+} concentration, the amount of SeNPs formed also increased due to the increase of Se active sites. However, a higher Se^{4+} concentration can lead to larger-sized particles due to their agglomeration and thus a decrease in process efficiency. When increasing the synthesis time from 2 to 4 h, the SeNP formation increased; after 4 h, the maximum absorbance of the SeNP solution insignificantly changed (Figure 1c). Up to 6 h, the SeNP formation efficiency decreased, and the plasmon band shifted to a higher wavelength region attributed to the agglomeration of SeNPs toward larger particles. Therefore, the synthesis time of 4 h should be chosen for further conditions. The biosynthesis of selenium nanoparticles was investigated at different temperatures (90−130 °C) (Figure 1d), indicating the suitable temperature of 120 °C with the highest absorbance intensity and lowest absorbance wavelength.

From the UV−vis spectral analysis, the suitable conditions for SeNP biosynthesis using orange peel extract as a reducing agent were determined, as follows: synthesis duration of 4 h, V_{Ext}/V_{Se} ratio of 40/10, Se^{4+} concentration of 80 mM, and reaction temperature of 120 °C.

The Characteristics of Selenium Nanoparticles. XRD analysis was performed to ensure the crystalline nature of the as-synthesized SeNPs at the optimized conditions (Figure 2a). The diffraction peaks at 2θ = 23.8, 29.5, 41.1, 45.1, 46.5, 48.0, 57.1, 61.1, 64.5, 65.7, 72.3, and 76.7° were recorded, corresponding to the (100), (101), (110), (102), (111), (200), (112), (202), (210), (211), (113), and (301) planes in the hexagonal phase of selenium crystals, being perfectly consistent with the pure phase of selenium (JCPDS Card No. 86-2246). Besides, a broad peak in the range of 20−30° was also detected, indicating the presence of carbon, related to

https://doi.org/10.1021/acsomega.2c05469
ACS Omega 2022, 7, 36037−36046

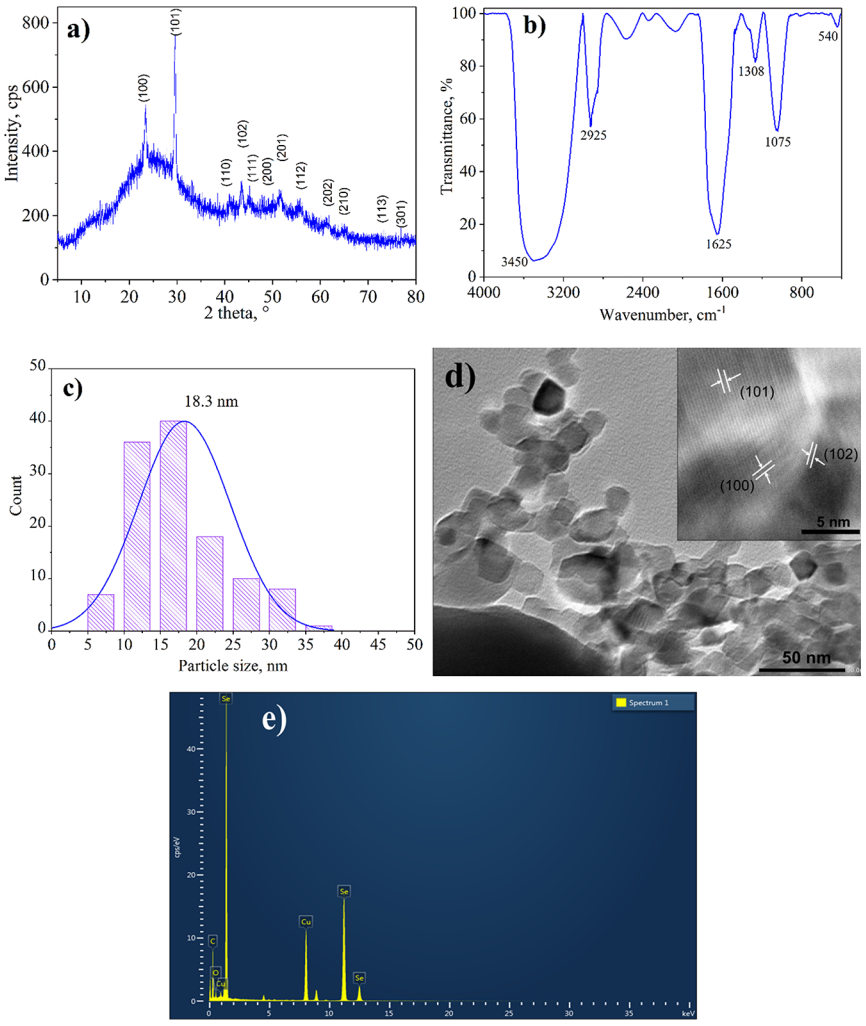

Figure 2. (a) XRD pattern, (b) FT-IR spectrum, (c) size distribution, (d) HR-TEM image, and (e) EDS spectrum of selenium nanoparticles synthesized at the optimized conditions.

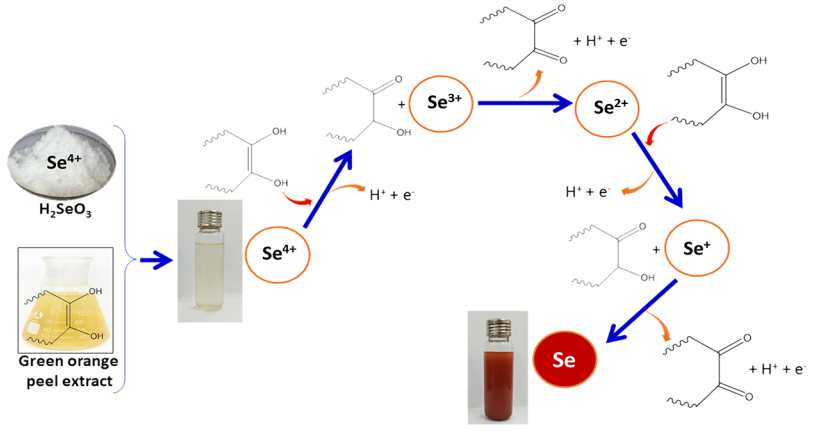

Figure 3. The synthesis mechanism of SeNPs using the GOP extract as a reducing agent.

phytochemical components of the orange peel extract (such as polyphenols, flavonoids, etc.), which are responsible for the reduction and stabilization of the formed SeNPs. The lattice parameter of as-prepared SeNPs was estimated via interplanar spacing (d-spacing) of the (101) plane at $2\theta = 29.5°$, as follows:

$$\alpha = d\sqrt{h^2 + k^2 + l^2} \quad (1)$$

where α is a lattice parameter [Å]; d is d-spacing [Å]; and h, k, and l are the Miller indices of the (101) crystal plane. A d-spacing value of 3.1 Å and a lattice parameter of 4.3 Å for the Miller indices corresponding to (101) plane matched well with the standard lattice parameter (α = 4.36 Å). The average

https://doi.org/10.1021/acsomega.2c05469
ACS Omega 2022, 7, 36037−36046

crystal size of SeNPs calculated by the Debye−Scherrer formula at $2\theta = 29.5°$ of the (101) plane is about 18.9 nm.

Figure 2b shows the FT-IR spectrum of SeNPs synthesized at the optimal condition using the GOP extract as a reducing agent. The abroad peak at 3450 cm^{-1} was related to the stretching vibrations of the O−H groups. The absorption peak at 2925 cm^{-1} was attributed to the C−H stretching of the aromatic compounds of the orange peel extract, the strong band at 1625 cm^{-1} corresponded to the stretching vibrations of the C═C aromatic bond of phenolic groups, and the peak at 1308 cm^{-1} was related to the bending vibrations of the CH_2 groups. The results confirmed the existence of polyphenols and flavonoid compounds in phytochemical compositions of the GOP extract. The presence of SeNPs was confirmed by the stretching vibrations of the terminal Se−O and O−Se−O groups at 1075 and 540 cm^{-1}, respectively.[19] The mechanism by which phytochemical compositions performed their reduction function to form SeNPs is described in Figure 3. A single selenium atom is tiny, but its surface free energy is very high. The aggregation of multiple selenium atoms can significantly reduce the surface free energy and become stable after the formation of particles. Besides, polyphenolic groups of the GOP have a strong steric effect on selenium and selenium ions; the biomolecules wrap around the surface of SeNPs and play an important role in their dispersion and protection. As the essence of protection, the encapsulation of phytochemicals reduces the surface free energy of SeNPs; the SeNPs become stable, preventing their agglomeration. The particle size distribution of SeNPs synthesized under optimal conditions is presented in Figure 2c, showing a range of 5−40 nm with the highest average intensity at 18.3 nm.

To study the morphology and size of the as-prepared SeNPs, the HR-TEM image is shown in Figure 2d, evidencing the formation of crystalline SeNPs with a spherical shape in the size range of 10−20 nm. Besides, a thin layer of biomolecules in the GOP extract around SeNPs could be observed, taking the role of preventing their agglomeration and enhancing their stability. Furthermore, SeNPs exhibited three crystal planes, including (101), (100), and (102) with d-spacing of 0.303, 0.290, and 0.300 nm, respectively. These results are completely consistent with the above analysis.

The EDS result (Figure 2e) revealed the presence of Se, C, O, and Cu in the SeNP samples with high intensities. The appearance of the O and C signals could be contributed by phytochemicals in the GOP extract covering the surface of SeNPs. Also, the C and Cu peaks could be related to the use of the carbon tape as a substrate. The mass percentages of Se, C, O, and Cu elements in SeNP samples were 59.6, 14.4, 1.4, and 24.4%, respectively.

The average particle size of as-prepared SeNPs using the GOP extract as a reducing agent was compared to those of other studies with similar protocols (Table 1). In the previous reports, various plants with their respective portions have been exploited, showing polydisperse SeNPs with wide ranges of variation. Compared with other green reducing agents and precursors, the SeNP sample synthesized from the GOP extract and H_2SeO_3 by the hydrothermal method also has a spherical shape, but the synthesis duration is shortened significantly, and at the same time, it has smaller size and higher uniformity.

Antibacterial Activity against MRSA. Figure 4 shows the inhibition zone of the as-synthesized SeNP sample against MRSA bacteria. It can be observed that there is almost no difference in inhibition diameter between the three investigations. The average inhibition zone diameter of the SeNP

Table 1. Comparison of Preparation Conditions and Particle Size of SeNPs Synthesized by Using Various Green Reducing Agents[a]

origin of reducing agents	selenium precursor	synthesis conditions	particle size, nm	refs
green orange peel	H_2SeO_3	hydrothermal at 120 °C for 4 h	5−40	this work
Diospyros montana		incubated at RT for 24 h	4−16	28
Vitis vinifera		refluxed for 15 min	3−18	32
Allium sativum		incubated at RT for 48 h	205	45
Capsicum annum		stirred at RT for 15 h	200−500	46
Acacia senegal		stirred at RT for 6 h	34.9	47
Brassica		stirred at RT for 12 h	50−150	48
orange peel	Na_2SeO_3	incubated at RT for 3 h	16−95	49
glucose		incubated at 90 °C for 12 h	32.3 ± 5.6	6
bee propolis		stirred at RT for 24 h	52−118	50
Aloe vera		shaken in the dark for 72 h	7−48	51
Terminalia arjuna		incubated at 30 °C for 72 h in dark conditions	10−80	52
Undaria pinnatifida		sonication condition for 5 min	44−94	53
Citrus limon		incubated at 30 °C for 24 h in the dark	60−80	54
Terminalia		shaken at 30 °C for 72 h in the dark	10−80	52
Citrus reticulata		stirred at 40 °C	70	55
Zingiber officinale		shaken at 30 °C for 72 h in dark conditions	10−20	56
parsley	$NaHSeO_3$	stayed overnight at RT	50−100	31
Bacillus licheniformis	SeO_2	incubated at 37 °C for 48 h	10−50	57
Aspergillus oryzae and gamma rays		incubated at RT for 24 h	55.0	58
chitosan and *Pleurotus ostreatus*		stirred at RT (24.0 ± 2 °C) for 20 min	27.35	30

[a]Note: RT, room temperature.

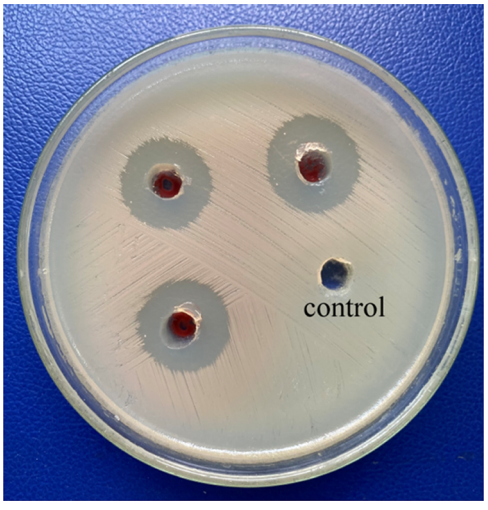

Figure 4. Inhibition zone of the synthesized SeNP solution against MRSA.

https://doi.org/10.1021/acsomega.2c05469
ACS Omega 2022, 7, 36037−36046

sample against MRSA bacteria was 20.0 ± 0.7 mm. For the MIC test (Figure 5), the delayed exponential phase of MRSA

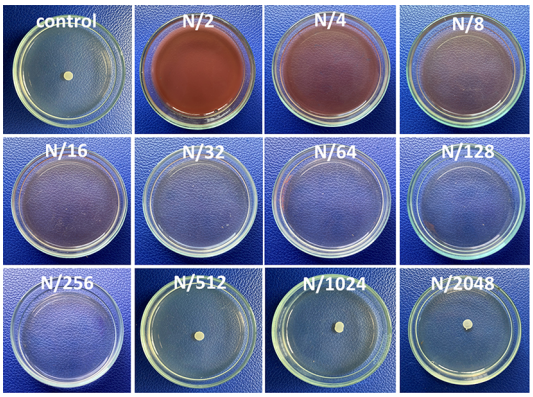

Figure 5. The minimum inhibitory concentration (MIC) of the synthesized SeNP solution against MRSA (N = 1.263 g/L).

in the presence of the SeNP solution was observed, and this phenomenon was more prominent with the growth in the SeNP concentration. The SeNP solution could inhibit the exponential phase of bacteria and completely inhibit the MRSA bacteria at an MIC of N/256 (4.94 μg/L).

The SeNP colloid synthesized from GOP has quite high antibacterial activity against MRSA compared to the metallic nanoparticles decorated on supports, the colloids of AgNPs and CuNPs, as well as the extract of *Quercus infectoria* Olivier nutgalls and leaves, leaves of *Melianthus comosus* Vahl, *Nymphaea lotus* Linn., and *Dodonaea angustifolia* (L.f.) Benth (shown in Table 2). Besides that, when the antibacterial zone sizes of the SeNPs and the antibiotics are compared, it is noticeable that the zone size of the SeNP sample is larger than that of the antibiotics including clindamycin, erythromycin, and ciprofloxacin and approximately equal to that of linezolid and gentamicin (as shown in Table 2). But the MIC value of SeNPs green-synthesized using the GOP extract is much lower than that of all five antibiotics. In contrast to commercial antibiotics, nanoparticles may be described by their primary benefits as antibacterial agents since they can operate multiple mechanisms, while bacteria cannot gain resistance to these indicated action methods.[59] Furthermore, these SeNPs demonstrated minimal or limited cytotoxicity against human dermal fibroblast, easing some of the safety concerns connected with the manufacturing procedure.[5] As a result, SeNPs appear to be trustworthy candidates for safe medicinal uses to prevent MRSA development.[60]

The antibacterial mechanism of SeNPs against MRSA is illustrated in Figure 6, including the direct adhesion of SeNPs to the bacterial surface and the effect on the structural integrity of the membrane.[73,74] Then, SeNPs enter the bacterial cell and interact with its internal components, causing it to become damaged to the point where it can no longer execute important cellular operations.[75] SeNPs could also generate reactive oxygen species and free radicals, causing irreversible oxidative damage to bacteria.[76] SeNPs impact critical signaling pathways, which are essential for the bacterial life cycle.[77]

The attachment of SeNPs to the membrane drastically changes both the membrane's permeability and structural integrity.[74] Electrostatic forces are created when positively charged SeNPs interface with negatively charged bacterial cell membranes.[78] The presence of the amino, carboxyl, and

Table 2. Comparison of Antibacterial Activity of the Green-Synthesized SeNPs against Methicillin-Resistant *Staphylococcus aureus* with Other Samples[a]

samples	IZD (mm)	MIC	refs
SeNPs	20.0 ± 0.7	4.94 μg/L	this work
α-/β-/γ-CuO@TiO_2	ND	1.50−2.33 mg/mL	61
AgNPs/$AgVO_3$	ND	6.75−12.5 μg/mL	62
AgNPs	10 ± 1 (20 ppm[b])	0.47 ± 0.27 ppm	63
ZnO	37 ± 2 (21%[b])	3.28 ± 0.55 ppm	63
mesoporous bioactive glass/Ag (the mole ratio of 90/10)	9.7 ± 0.4	10 mg/mL	64
AgNPs biosynthesized by *Bacillus subtilis* bacteria	ND	230 μg/mL	65
AgNPs synthesized with thymol or usnic acid as reducer/stabilizer	12.9−13.8	60 μg/L	66
CuNPs synthesized with thymol or usnic acid as reducer/stabilizer	22.8−26.7	40 μg/L	66
AuNPs synthesized from *G. elongata* ethanol extract	16	ND	67
Melianthus comosus Vahl leaves extract	ND	0.39 mg/mL	68
Dodonaea angustifolia (L.f.) Benth leaves extract	ND	0.59 mg/mL	68
Quercus infectoria Olivier nutgalls extract	ND	0.4−3.2 mg/mL	69
Nymphaea lotus Linn. leaf extract	ND	5.0−10.0 mg/mL	70
vancomycin	ND	1.56 ± 0.23 μg/mL	71
linezolid	21	30 μg/mL	72
gentamicin	21	10 μg/mL	72
clindamycin	15	2 μg/mL	72
erythromycin	12	15 μg/mL	72
ciprofloxacin	15	5 μg/mL	72

[a]Note: inhibition zone diameter (IZD), ; MIC, minimum inhibitory concentration; ND, not done. [b]Concentration used for the inhibition zone diameter test.

phosphate groups contributes significantly to explain why the membrane is negatively charged.[79] Several experiments on bacteria using transmission electron microscopes have shown that SeNPs permeate the cells, supporting this claim.[80,81] Furthermore, in the presence of oxygen and proton, SeNPs break down to ions, making infusion easier.[82] When SeNPs enter the cell, they interact with biological components and structures such as proteins, deoxyribonucleic acid (DNA), and lipids.[83] For example, SeNPs disrupt protein synthesis by binding with the ribosome and denaturing it, causing the translation process to cease.[84] SeNPs also interact with DNA molecules, which can result in DNA denaturation and shearing, as well as cell division disruption.[85] The interaction renders the bacteria incapable of cell division and reproduction, ultimately leading to death.

The reactive oxygen species (ROS) are also the perpetrators of bacterial growth suppression.[86] SeNPs produce a high quantity of ROS, causing oxidative stress in the cell.[87] The destruction of major cellular components such as proteins, DNA, and ribonucleic acid (RNA) caused by oxidative stress results in altered membrane permeability and increased biological component leakage from the cell.[88] The bacteria will suffer permanent oxidative damage and cell death as a

https://doi.org/10.1021/acsomega.2c05469
ACS Omega 2022, 7, 36037−36046

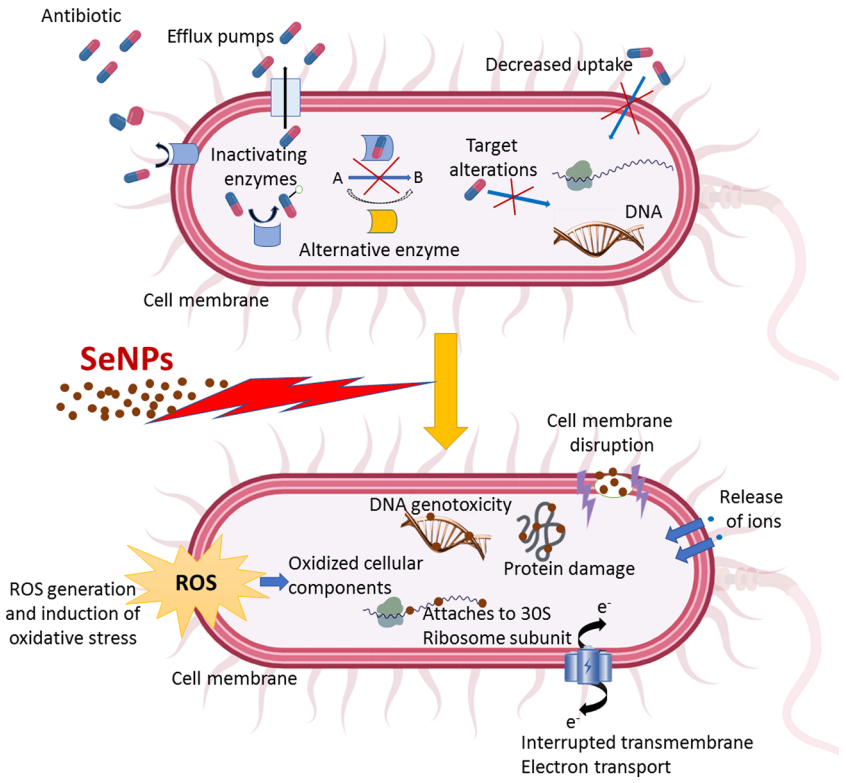

Figure 6. The illustration of the antibacterial mechanism of SeNPs against MRSA.

result of this.[89] SeNPs are thought to be effective against MRSA because they demonstrate several modes of action on bacteria.

CONCLUSIONS

Green nanotechnology is gaining importance, eliminating harmful reagents and providing cost-effective protocols of expected products. This study established a rapid, simple, inexpensive, and eco-friendly approach to produce SeNPs using the GOP extract as reducing and stabilizing agents (byproduct of the orange manufacturing industry). At the optimal conditions, the as-prepared SeNPs were found to have a highly crystallized spherical shape and an average size of 18.3 nm, with high stability thanks to the encapsulation of phytochemicals in the green orange peel extract and the prevention of agglomeration. The wide inhibition zone and low MIC values against MRSA of SeNP samples indicated their good antibacterial activity. Green-synthesized SeNPs in this work could be a promising approach for the treatment of diseases caused by drug-resistant strains.

AUTHOR INFORMATION

Corresponding Authors

Phan Hong Phuong − *Ho Chi Minh City University of Technology (HCMUT), Ho Chi Minh City 700000, Vietnam; Vietnam National University Ho Chi Minh City, Ho Chi Minh City 700000, Vietnam*; Email: phphuongdk@hcmut.edu.vn

Tri Nguyen − *Institute of Chemical Technology-VAST, Ho Chi Minh City 700000, Vietnam; Ho Chi Minh City Open University, Ho Chi Minh City 700000, Vietnam*; orcid.org/0000-0001-9486-5096; Email: ntri@ict.vast.vn

Authors

Trung Dang-Bao − *Ho Chi Minh City University of Technology (HCMUT), Ho Chi Minh City 700000, Vietnam; Vietnam National University Ho Chi Minh City, Ho Chi Minh City 700000, Vietnam*

Thanh Gia-Thien Ho − *Institute of Chemical Technology-VAST, Ho Chi Minh City 700000, Vietnam*

Ba Long Do − *Institute of Chemical Technology-VAST, Ho Chi Minh City 700000, Vietnam*

Nguyen Phung Anh − *Institute of Chemical Technology-VAST, Ho Chi Minh City 700000, Vietnam*

Thi Diem Trinh Phan − *Ho Chi Minh City Open University, Ho Chi Minh City 700000, Vietnam*

Thi Bao Yen Tran − *Ho Chi Minh City Open University, Ho Chi Minh City 700000, Vietnam*

Nhat Linh Duong − *Ho Chi Minh City Open University, Ho Chi Minh City 700000, Vietnam*

Complete contact information is available at: https://pubs.acs.org/10.1021/acsomega.2c05469

Notes

The authors declare no competing financial interest.

ACKNOWLEDGMENTS

We acknowledge the support in the form of time and facilities from Ho Chi Minh University of Technology (HCMUT), VNU-HCM, for this study.

REFERENCES

(1) Korde, P.; Ghotekar, S.; Pagar, T.; Pansambal, S.; Oza, R.; Mane, D. Plant extract assisted eco-benevolent synthesis of selenium nanoparticles-a review on plant parts involved, characterization and their recent applications. *J. Chem. Rev.* **2020**, *2*, 157−168.

(2) Hosnedlova, B.; Kepinska, M.; Skalickova, S.; Fernandez, C.; Ruttkay-Nedecky, B.; Peng, Q.; Baron, M.; Melcova, M.; Opatrilova, R.; Zidkova, J.; Bjørklund, G.; Sochor, J.; Kizek, R. Nano-selenium and its nanomedicine applications: a critical review. *Int. J. Nanomed.* **2018**, *Volume 13*, 2107.
(3) Khurana, A.; Tekula, S.; Saifi, M. A.; Venkatesh, P.; Godugu, C. Therapeutic applications of selenium nanoparticles. *Biomed. Pharmacother.* **2019**, *111*, 802−812.
(4) Wen, S.; Hui, Y.; Chuang, W. Biosynthesis and antioxidation of nano-selenium using lemon juice as a reducing agent. *Green Process. Synth.* **2021**, *10*, 178−188.
(5) Medina Cruz, D.; Mi, G.; Webster, T. J. Synthesis and characterization of biogenic selenium nanoparticles with antimicrobial properties made by *Staphylococcus aureus*, methicillin-resistant *Staphylococcus aureus* (MRSA), *Escherichia coli*, and *Pseudomonas aeruginosa*. *J. Biomed. Mater. Res.* **2018**, *106*, 1400−1412.
(6) Han, H.-W.; Patel, K. D.; Kwak, J.-H.; Jun, S.-K.; Jang, T.-S.; Lee, S.-H.; Knowles, J. C.; Kim, H.-W.; Lee, H.-H.; Lee, J.-H. Selenium nanoparticles as candidates for antibacterial substitutes and supplements against multidrug-resistant bacteria. *Biomolecules* **2021**, *11*, 1028.
(7) Masimen, M. A. A.; Harun, N. A.; Maulidiani, M.; Ismail, W. I. W. Overcoming Methicillin-resistance *Staphylococcus aureus* (MRSA) using antimicrobial peptides-silver nanoparticles. *Antibiotics* **2022**, *11*, 951.
(8) Brown, N. M.; Goodman, A. L.; Horner, C.; Jenkins, A.; Brown, E. M. Treatment of methicillin-resistant *Staphylococcus aureus* (MRSA): updated guidelines from the UK. *JAC Antimicrob. Resist.* **2021**, *3*, dlaa114.
(9) Murugesan, G.; Nagaraj, K.; Sunmathi, D.; Subramani, K. Methods involved in the synthesis of selenium nanoparticles and their different applications-a review. *Eur. J. Biomed.* **2019**, *6*, 189−194.
(10) Rajeshkumar, S.; Veena, P.; Santhiyaa, R., Synthesis and characterization of selenium nanoparticles using natural resources and its applications. In *Exploring the Realms of Nature for Nanosynthesis*, Springer: 2018; pp. 63−79.
(11) Charlet, L.; Scheinost, A. C.; Tournassat, C.; Greneche, J.-M.; Géhin, A.; Fernández-Martı, A.; Coudert, S.; Tisserand, D.; Brendle, J. Electron transfer at the mineral/water interface: Selenium reduction by ferrous iron sorbed on clay. *Geochim. Cosmochim. Acta* **2007**, *71*, 5731−5749.
(12) Kumar, A.; Sevonkaev, I.; Goia, D. V. Synthesis of selenium particles with various morphologies. *J. Colloid Interface Sci.* **2014**, *416*, 119−123.
(13) Lin, Z.-H.; Wang, C. R. C. Evidence on the size-dependent absorption spectral evolution of selenium nanoparticles. *Mater. Chem. Phys.* **2005**, *92*, 591−594.
(14) Wang, T.; Wang, Q.; Wang, Y.; Da, Y.; Zhou, W.; Shao, Y.; Li, D.; Zhan, S.; Yuan, J.; Wang, H. Atomically dispersed semimetallic selenium on porous carbon membrane as an electrode for hydrazine fuel cells. *Am. Ethnol.* **2019**, *131*, 13600−13605.
(15) Zou, X.; Jiang, Z.; Li, L.; Huang, Z. Selenium nanoparticles coated with pH responsive silk fibroin complex for fingolimod release and enhanced targeting in thyroid cancer. *Artif. Cells Nanomed. Biotechnol.* **2021**, *49*, 83−95.
(16) Siddiqui, S. A.; Blinov, A. V.; Serov, A. V.; Gvozdenko, A. A.; Kravtsov, A. A.; Nagdalian, A. A.; Raffa, V. V.; Maglakelidze, D. G.; Blinova, A. A.; Kobina, A. V.; Golik, A. B.; Ibrahim, S. A. Effect of selenium nanoparticles on germination of hordéum vulgáre barley seeds. *Coatings* **2021**, *11*, 862.
(17) Cao, H.; Yang, Y.; Chen, X.; Liu, J.; Chen, C.; Yuan, S.; Yu, L. Synthesis of selenium-doped carbon from glucose: An efficient antibacterial material against Xcc. *Chin. Chem. Lett.* **2020**, *31*, 1887−1889.
(18) Shi, X.-D.; Tian, Y.-Q.; Wu, J.-L.; Wang, S.-Y. Synthesis, characterization, and biological activity of selenium nanoparticles conjugated with polysaccharides. *Crit. Rev. Food Sci. Nutr.* **2021**, *61*, 2225−2236.
(19) Shirmehenji, R.; Javanshir, S.; Honarmand, M. A green approach to the bio-based synthesis of selenium nanoparticles from mining waste. *J. Cluster Sci.* **2021**, *32*, 1311−1323.
(20) Ojeda, J. J.; Merroun, M. L.; Tugarova, A. V.; Lampis, S.; Kamnev, A. A.; Gardiner, P. H. Developments in the study and applications of bacterial transformations of selenium species. *Crit. Rev. Biotechnol.* **2020**, *40*, 1250−1264.
(21) Reddy, B.; Bandi, R., Synthesis of selenium nanoparticles by using microorganisms and agri-based products. In *Agri-waste and microbes for production of sustainable nanomaterials*, Elsevier: 2022; pp. 655−683.
(22) Ye, Y.; Qu, J.; Pu, Y.; Rao, S.; Xu, F.; Wu, C. Selenium biofortification of crop food by beneficial microorganisms. *J. Fungi* **2020**, *6*, 59.
(23) Alagesan, V.; Venugopal, S. Green synthesis of selenium nanoparticle using leaves extract of *Withania somnifera* and its biological applications and photocatalytic activities. *Bionanoscience* **2019**, *9*, 105−116.
(24) Gunti, L.; Dass, R. S.; Kalagatur, N. K. Phytofabrication of selenium nanoparticles from *Emblica officinalis* fruit extract and exploring its biopotential applications: antioxidant, antimicrobial, and biocompatibility. *Front. Microbiol.* **2019**, *10*, 931.
(25) Alam, H.; Khatoon, N.; Khan, M. A.; Husain, S. A.; Saravanan, M.; Sardar, M. Synthesis of selenium nanoparticles using Probiotic Bacteria Lactobacillus acidophilus and their enhanced antimicrobial activity against resistant bacteria. *J. Cluster Sci.* **2020**, *31*, 1003−1011.
(26) Chandramohan, S.; Sundar, K.; Muthukumaran, A. Monodispersed spherical shaped selenium nanoparticles (SeNPs) synthesized by *Bacillus subtilis* and its toxicity evaluation in zebrafish embryos. *Mater. Res. Express* **2018**, *5*, No. 025020.
(27) Krausova, G.; Kana, A.; Hyrslova, I.; Mrvikova, I.; Kavkova, M. Development of selenized lactic acid bacteria and their selenium bioaccummulation capacity. *Fermentation* **2020**, *6*, 91.
(28) Kokila, K.; Elavarasan, N.; Sujatha, V. Diospyros montana leaf extract-mediated synthesis of selenium nanoparticles and their biological applications. *New J. Chem.* **2017**, *41*, 7481−7490.
(29) Tian, M.; Yang, Y.; Ávila, F. W.; Fish, T.; Yuan, H.; Hui, M.; Pan, S.; Thannhauser, T. W.; Li, L. Effects of selenium supplementation on glucosinolate biosynthesis in broccoli. *J. Agric. Food Chem.* **2018**, *66*, 8036−8044.
(30) El-Batal, A. I.; Mosallam, F. M.; Ghorab, M.; Hanora, A.; Gobara, M.; Baraka, A.; Elsayed, M. A.; Pal, K.; Fathy, R. M.; Abd Elkodous, M.; El-Sayyad, G. S. Factorial design-optimized and gamma irradiation-assisted fabrication of selenium nanoparticles by chitosan and *Pleurotus ostreatus* fermented fenugreek for a vigorous in vitro effect against carcinoma cells. *Int. J. Biol. Macromol.* **2020**, *156*, 1584−1599.
(31) Fritea, L.; Laslo, V.; Cavalu, S.; Costea, T.; Vicas, S. I. Green biosynthesis of selenium nanoparticles using *Parsley* (*Petroselinum crispum*) leaves extract. *Studia Univ. Vasile Goldis Arad, Ser. Stiintele Vietii* **2017**, *27*, 203−208.
(32) Sharma, G.; Sharma, A. R.; Bhavesh, R.; Park, J.; Ganbold, B.; Nam, J.-S.; Lee, S.-S. Biomolecule-mediated synthesis of selenium nanoparticles using dried *Vitis vinifera (raisin)* extract. *Molecules* **2014**, *19*, 2761−2770.
(33) Kumar, A.; Prasad, K. S. Role of nano-selenium in health and environment. *J. Biotechnol.* **2021**, *325*, 152−163.
(34) Sowndarya, P.; Ramkumar, G.; Shivakumar, M. S. Green synthesis of selenium nanoparticles conjugated *Clausena dentata* plant leaf extract and their insecticidal potential against mosquito vectors. *Artif. Cells Nanomed. Biotechnol.* **2017**, *45*, 1490−1495.
(35) Fardsadegh, B.; Jafarizadeh-Malmiri, H. *Aloe vera* leaf extract mediated green synthesis of selenium nanoparticles and assessment of their in vitro antimicrobial activity against spoilage fungi and pathogenic bacteria strains. *Green Process. Synth.* **2019**, *8*, 399−407.
(36) Bátori, V.; Jabbari, M.; Åkesson, D.; Lennartsson, P. R.; Taherzadeh, M. J.; Zamani, A. Production of pectin-cellulose biofilms: a new approach for citrus waste recycling. *Int. J. Polym. Sci.* **2017**, *2017*, 1.

https://doi.org/10.1021/acsomega.2c05469
ACS Omega 2022, 7, 36037−36046

(37) Skiba, M. I.; Vorobyova, V. I. Synthesis of silver nanoparticles using orange peel extract prepared by plasmochemical extraction method and degradation of methylene blue under solar irradiation. *Adv. Mater. Sci. Eng.* **2019**, *2019*, 1.
(38) Tanase, C.; Coşarcă, S.; Muntean, D.-L. A critical review of phenolic compounds extracted from the bark of woody vascular plants and their potential biological activity. *Molecules* **2019**, *24*, 1182.
(39) Singleton, V. L.; Orthofer, R.; Lamuela-Raventós, R. M. Analysis of total phenols and other oxidation substrates and antioxidants by means of folin-ciocalteu reagent. *Methods Enzymol.* **1999**, *299*, 152−178.
(40) Turkmen, N.; Velioglu, Y.; Sari, F.; Polat, G. Effect of extraction conditions on measured total polyphenol contents and antioxidant and antibacterial activities of black tea. *Molecules* **2007**, *12*, 484−496.
(41) Vuong, Q. V.; Hirun, S.; Roach, P. D.; Bowyer, M. C.; Phillips, P. A.; Scarlett, C. J. Effect of extraction conditions on total phenolic compounds and antioxidant activities of *Carica papaya* leaf aqueous extracts. *J. Herb. Med.* **2013**, *3*, 104−111.
(42) Sulaiman, I. S. C.; Basri, M.; Masoumi, H. R. F.; Chee, W. J.; Ashari, S. E.; Ismail, M. Effects of temperature, time, and solvent ratio on the extraction of phenolic compounds and the anti-radical activity of *Clinacanthus nutans Lindau* leaves by response surface methodology. *Chem. Cent. J.* **2017**, *11*, 1−11.
(43) Essien, E. E. Effect of extraction conditions on total polyphenol contents, antioxidant and antimicrobial activities of *Cannabis sativa L. Elec. J. Env. Agricult. Food Chem.* **2011**, *11*, 300−307.
(44) Naczk, M.; Shahidi, F. Extraction and analysis of phenolics in food. *J. Chromatogr. A* **2004**, *1054*, 95−111.
(45) Ezhuthupurakkal, P. B.; Polaki, L. R.; Suyavaran, A.; Subastri, A.; Sujatha, V.; Thirunavukkarasu, C. Selenium nanoparticles synthesized in aqueous extract of *Allium sativum* perturbs the structural integrity of Calf thymus DNA through intercalation and groove binding. *Mater. Sci. Eng. C* **2017**, *74*, 597−608.
(46) Li, S.; Shen, Y.; Xie, A.; Yu, X.; Zhang, X.; Yang, L.; Li, C. Rapid, room-temperature synthesis of amorphous selenium/protein composites using *Capsicum annuum L.* extract. *Nanotechnology* **2007**, *18*, 405101.
(47) Kong, H.; Yang, J.; Zhang, Y.; Fang, Y.; Nishinari, K.; Phillips, G. O. Synthesis and antioxidant properties of gum arabic-stabilized selenium nanoparticles. *Int. J. Biol. Macromol.* **2014**, *65*, 155−162.
(48) Kapur, M.; Soni, K.; Kohli, K. Green synthesis of selenium nanoparticles from broccoli, characterization, application and toxicity. *Adv. Tech. Biol. Med* **2017**, *05*, 2379−1764.
(49) Salem, S. S.; Badawy, M. S. E.; Al-Askar, A. A.; Arishi, A. A.; Elkady, F. M.; Hashem, A. H. Green biosynthesis of selenium nanoparticles using orange peel waste: Characterization, antibacterial and antibiofilm activities against multidrug-resistant bacteria. *Life* **2022**, *12*, 893.
(50) Shubharani, R.; Mahesh, M.; Yogananda Murthy, V. Biosynthesis and characterization, antioxidant and antimicrobial activities of selenium nanoparticles from ethanol extract of Bee Propolis. *J. Nanomed. Nanotechnol.* **2019**, *10*, 2.
(51) Vyas, J.; Rana, S. Antioxidant activity and biogenic synthesis of selenium nanoparticles using the leaf extract of *Aloe vera*. *Int. J. Curr. Pharm. Res.* **2017**, *9*, 147−152.
(52) Prasad, K. S.; Selvaraj, K. Biogenic synthesis of selenium nanoparticles and their effect on As (III)-induced toxicity on human lymphocytes. *Biol. Trace Elem. Res.* **2014**, *157*, 275−283.
(53) Chen, T.; Wong, Y.-S.; Zheng, W.; Bai, Y.; Huang, L. Selenium nanoparticles fabricated in *Undaria pinnatifida* polysaccharide solutions induce mitochondria-mediated apoptosis in A375 human melanoma cells. *Colloids Surf., B* **2008**, *67*, 26−31.
(54) Prasad, K. S.; Patel, H.; Patel, T.; Patel, K.; Selvaraj, K. Biosynthesis of Se nanoparticles and its effect on UV-induced DNA damage. *Colloids Surf., B* **2013**, *103*, 261−266.
(55) Santanu, S.; Sowmiya, R.; Balakrishnaraja, R. Biosynthesis of selenium nanoparticles using *Citrus reticulata* peel extract. *World J. Pharm. Res.* **2015**, *4*, 1322−1330.
(56) Zahran, W. E.; Elsonbaty, S. M.; Moawed, F. S. M. Selenium nanoparticles with low-level ionizing radiation exposure ameliorate nicotine-induced inflammatory impairment in rat kidney. *Environ. Sci. Pollut. Res.* **2017**, *24*, 19980−19989.
(57) Khiralla, G. M.; El-Deeb, B. A. Antimicrobial and antibiofilm effects of selenium nanoparticles on some foodborne pathogens. *LWT−Food Sci. Technol.* **2015**, *63*, 1001−1007.
(58) Mosallam, F. M.; El-Sayyad, G. S.; Fathy, R. M.; El-Batal, A. I. Biomolecules-mediated synthesis of selenium nanoparticles using *Aspergillus oryzae* fermented *Lupin* extract and gamma radiation for hindering the growth of some multidrug-resistant bacteria and pathogenic fungi. *Microb. Pathog.* **2018**, *122*, 108−116.
(59) Filipović, N.; Ušjak, D.; Milenković, M. T.; Zheng, K.; Liverani, L.; Boccaccini, A. R.; Stevanović, M. M. Comparative study of the antimicrobial activity of selenium nanoparticles with different surface chemistry and structure. *Front. Bioeng. Biotechnol* **2021**, *8*, 624621.
(60) Rai, M.; Ingle, A. P.; Pandit, R.; Paralikar, P.; Gupta, I.; Chaud, M. V.; dos Santos, C. A. Broadening the spectrum of small-molecule antibacterials by metallic nanoparticles to overcome microbial resistance. *Int. J. Pharm.* **2017**, *532*, 139−148.
(61) Baig, U.; Ansari, M. A.; Gondal, M.; Akhtar, S.; Khan, F. A.; Falath, W. Single step production of high-purity copper oxide-titanium dioxide nanocomposites and their effective antibacterial and anti-biofilm activity against drug-resistant bacteria. *Mater. Sci. Eng. C.* **2020**, *113*, 110992.
(62) Holtz, R. D.; Souza Filho, A.; Brocchi, M.; Martins, D.; Durán, N.; Alves, O. Development of nanostructured silver vanadates decorated with silver nanoparticles as a novel antibacterial agent. *Nanotechnology* **2010**, *21*, 185102.
(63) Rezić, I.; Majdak, M.; Ljoljić Bilić, V.; Pokrovac, I.; Martinaga, L.; Somogyi Škoc, M.; Kosalec, I. Development of antibacterial protective coatings active against MSSA and MRSA on biodegradable polymers. *Polymer* **2021**, *13*, 659.
(64) Chen, Y.-H.; Kung, J.-C.; Tseng, S.-P.; Chen, W.-C.; Wu, S.-M.; Shih, C.-J. Effects of AgNPs on the structure and anti-methicillin resistant *Staphylococcus aureus* (MRSA) properties of SiO_2-CaO-P_2O_5 bioactive glass. *J. Non-Cryst. Solids* **2021**, *553*, 120492.
(65) Alsamhary, K. I. Eco-friendly synthesis of silver nanoparticles by *Bacillus subtilis* and their antibacterial activity. *Saudi J. Biol. Sci.* **2020**, *27*, 2185−2191.
(66) Alavi, M.; Karimi, N. Biosynthesis of Ag and Cu NPs by secondary metabolites of usnic acid and thymol with biological macromolecules aggregation and antibacterial activities against multi drug resistant (MDR) bacteria. *Int. J. Biol. Macromol.* **2019**, *128*, 893−901.
(67) Abdel-Raouf, N.; Al-Enazi, N. M.; Ibraheem, I. B. M. Green biosynthesis of gold nanoparticles using *Galaxaura elongata* and characterization of their antibacterial activity. *Arab. J. Chem.* **2017**, *10*, S3029−S3039.
(68) Heyman, H. M.; Hussein, A. A.; Meyer, J. J. M.; Lall, N. Antibacterial activity of South African medicinal plants against methicillin resistant *Staphylococcus aureus*. *Pharm. Biol.* **2009**, *47*, 67−71.
(69) Sucilathangam, G.; Gomatheswari, S.; Velvizhi, G.; Vincent, C.; Palaniappan, N. Detection of anti-bacterial activity of medicinal plant Quercus infectoria against MRSA isolates in clinical samples. *J. Pharm. Biomed.* **2012**, *14*, 1−4.
(70) Akinjogunla, O. J.; Yah, C. S.; Eghafona, N. O.; Ogbemudia, F. O. Antibacterial activity of leave extracts of *Nymphaea lotus* (*Nymphaeaceae*) on methicillin resistant *Staphylococcus aureus* (MRSA) and vancomycin resistant *Staphylococcus aureus* (VRSA) isolated from clinical samples. *Ann. Biol. Res.* **2010**, *1*, 174−184.
(71) Awad, M.; Yosri, M.; Abdel-Aziz, M. M.; Younis, A. M.; Sidkey, N. M. Assessment of the antibacterial potential of biosynthesized silver nanoparticles combined with vancomycin against methicillin-resistant *Staphylococcus aureus*−Induced infection in rats. *Biol. Trace Elem. Res.* **2021**, *199*, 4225−4236.
(72) Manipriya, B.; Tasneem, B. A. N. U.; Prem, K. L.; Kalyani, M. Evaluation of antibacterial activity of silver nanoparticles against

https://doi.org/10.1021/acsomega.2c05469
ACS Omega 2022, 7, 36037−36046

methicillin-resistant *Staphylococcus aureus* and detection of virulence factors - nuclease, phosphatase, and bio film production. *Asian J. Pharm. Clin. Res.* **2018**, *11*, 224−229.
(73) Liu, W.; Golshan, N. H.; Deng, X.; Hickey, D. J.; Zeimer, K.; Li, H.; Webster, T. J. Selenium nanoparticles incorporated into titania nanotubes inhibit bacterial growth and macrophage proliferation. *Nanoscale* **2016**, *8*, 15783−15794.
(74) Huang, X.; Chen, X.; Chen, Q.; Yu, Q.; Sun, D.; Liu, J. Investigation of functional selenium nanoparticles as potent antimicrobial agents against superbugs. *Acta Biomater.* **2016**, *30*, 397−407.
(75) Palomo-Siguero, M.; Gutiérrez, A. M.; Pérez-Conde, C.; Madrid, Y. Effect of selenite and selenium nanoparticles on lactic bacteria: A multi-analytical study. *Microchem. J.* **2016**, *126*, 488−495.
(76) Hariharan, S.; Dharmaraj, S. Selenium and selenoproteins: It's role in regulation of inflammation. *Inflammopharmacology* **2020**, *28*, 667−695.
(77) Galić, E.; Ilić, K.; Hartl, S.; Tetyczka, C.; Kasemets, K.; Kurvet, I.; Milić, M.; Barbir, R.; Pem, B.; Erceg, I.; Dutour Sikirić, M.; Pavičić, I.; Roblegg, E.; Kahru, A.; Vinković Vrček, I. Impact of surface functionalization on the toxicity and antimicrobial effects of selenium nanoparticles considering different routes of entry. *Food Chem. Toxicol.* **2020**, *144*, 111621.
(78) Abou Elmaaty, T.; Sayed-Ahmed, K.; Elsisi, H.; Ramadan, S. M.; Sorour, H.; Magdi, M.; Abdeldayem, S. A. Novel antiviral and antibacterial durable polyester fabrics printed with selenium nanoparticles (SeNPs). *Polymer* **2022**, *14*, 955.
(79) Wang, X.; Song, W.; Qian, H.; Zhang, D.; Pan, X.; Gadd, G. M. Stabilizing interaction of exopolymers with nano-Se and impact on mercury immobilization in soil and groundwater. *Environ. Sci. Nano* **2018**, *5*, 456−466.
(80) Tan, H. W.; Mo, H.-Y.; Lau, A. T.; Xu, Y.-M. Selenium species: current status and potentials in cancer prevention and therapy. *Int. J. Mol. Sci.* **2019**, *20*, 75.
(81) Jahan, M. I.; Juengwiwattanakitti, P.; Izu, Y.; Tobe, R.; Imai, T.; Mihara, H. Selenite uptake by outer membrane porin ExtI and its involvement in the subcellular localization of rhodanese-like lipoprotein ExtH in Geobacter sulfurreducens. *Biochem. Biophys. Res. Commun.* **2019**, *516*, 474−479.
(82) Adebayo, E. A.; Oladipo, I. C.; Badmus, J. A.; Lateef, A. Beneficial Microbes as novel microbial cell factories in nanobiotechnology: potentials in nanomedicine. *Microb. Nanobiotechnol.* **2021**, 315−342.
(83) Escobar-Ramírez, M. C.; Castañeda-Ovando, A.; Pérez-Escalante, E.; Rodríguez-Serrano, G. M.; Ramírez-Moreno, E.; Quintero-Lira, A.; Contreras-López, E.; Añorve-Morga, J.; Jaimez-Ordaz, J.; González-Olivares, L. G. Antimicrobial activity of Se-nanoparticles from bacterial biotransformation. *Fermentation* **2021**, *7*, 130.
(84) Ikram, M.; Javed, B.; Raja, N. I.; Mashwani, Z. U. R. Biomedical potential of plant-based selenium nanoparticles: a comprehensive review on therapeutic and mechanistic aspects. *Int. J. Nanomed.* **2021**, *Volume 16*, 249.
(85) Fang, J.-Y.; Lin, Y.-K.; Wang, P.-W.; Alalaiwe, A.; Yang, Y.-C.; Yang, S.-C. The droplet-size effect of squalene@cetylpyridinium chloride nanoemulsions on antimicrobial potency against planktonic and biofilm MRSA. *Int. J. Nanomed.* **2019**, *14*, 8133.
(86) Kim, H. Y.; Go, J.; Lee, K.-M.; Oh, Y. T.; Yoon, S. S. Guanosine tetra-and pentaphosphate increase antibiotic tolerance by reducing reactive oxygen species production in Vibrio cholerae. *J. Biol. Chem.* **2018**, *293*, 5679−5694.
(87) Xiao, Y.; Zhang, X.; Huang, Q. Protective effects of *Cordyceps sinensis* exopolysaccharide-selenium nanoparticles on H_2O_2-induced oxidative stress in HepG2 cells. *Int. J. Biol. Macromol.* **2022**, *213*, 339−351.
(88) Juan, C. A.; Pérez de la Lastra, J. M.; Plou, F. J.; Pérez-Lebeña, E. The chemistry of reactive oxygen species (ROS) revisited: outlining their role in biological macromolecules (DNA, lipids and proteins) and induced pathologies. *Int. J. Mol. Sci.* **2021**, *22*, 4642.
(89) Lee, W.; Woo, E.-R.; Lee, D. G. Phytol has antibacterial property by inducing oxidative stress response in *Pseudomonas aeruginosa*. *Free Radical Res.* **2016**, *50*, 1309−1318.

https://doi.org/10.1021/acsomega.2c05469
ACS Omega 2022, 7, 36037−36046